11898 *J. Phys. Chem. A* **2009,** *113,* 11898–11906

Local Hybrid Functionals with an Explicit Dependence on Spin Polarization†

Alexei V. Arbuznikov,* Hilke Bahmann, and Martin Kaupp*

Institut für Anorganische Chemie, Universität Würzburg, D-97074 Würzburg, Germany

Received: April 8, 2009; Revised Manuscript Received: June 14, 2009

A new family of local hybrid functionals with a position-dependent mixture of local and exact exchange has been constructed. On the basis of conceptual similarities between local hybrids and explicit nondynamical correlation functionals, the relative spin polarization has been introduced as an additional variable into the local mixing function (LMF) that determines the position dependence of the exact exchange admixture. This leads to two new two-parameter LMFs, one based on the ratio of the local kinetic energy density to the von Weizsäcker kinetic energy density and the other on the dimensionless density gradient. After optimization of the two free parameters for small test sets, significant improvements of atomization energies of the full G3 set are obtained (mean absolute errors of 2.96 and 3.18 kcal mol^{-1}, respectively), with minor deterioration for classical reaction barriers (HTBH38 and NHTBH38 test sets). The simultaneous description of two-center three-electron dimer cations remains a challenge. It is shown that the exact and local spin density exchange energy densities have closely related gauge definitions, so that gauge mismatch is only a minor problem for local hybrids based on local exchange.

I. Introduction

The ability of hybrid exchange-correlation functionals to describe various properties of different physicochemical systems with high accuracy at low computational cost has made them the most successful and popular class of density functionals in a wide range of applications from chemistry via materials research to biophysics. The B3LYP[1–3] hybrid functional is nowadays well-known to every computational chemist and to most experimentalists as well. A typical hybrid functional is written as

$$E_{\mathrm{xc}}^{\mathrm{hybr}} = a_0 E_{\mathrm{x}}^{\mathrm{exact}} + \tilde{E}_{\mathrm{xc}}^{\mathrm{DFT}} \qquad 0 \le a_0 \le 1 \tag{1}$$

where $E_{\mathrm{x}}^{\mathrm{exact}}$ is the exact exchange (EXX) energy

$$E_{\mathrm{x}}^{\mathrm{exact}} = -\frac{1}{2}\sum_{\sigma=\alpha,\beta}\sum_{i,j}^{\mathrm{occ}}\int \frac{\varphi_{i_\sigma}^{*}(\mathbf{r})\varphi_{j_\sigma}^{*}(\mathbf{r}')\varphi_{j_\sigma}(\mathbf{r})\varphi_{i_\sigma}(\mathbf{r}')}{|\mathbf{r}-\mathbf{r}'|}\mathrm{d}\mathbf{r}\mathrm{d}\mathbf{r}' \tag{2}$$

and $\tilde{E}_{\mathrm{xc}}^{\mathrm{DFT}}$ is some (physically justified) linear combination of "traditional" density functionals, usually based either on the local spin density approximation (LSDA)[4–6] or on the generalized gradient approximation (GGA).[2,7–10] The simplest form of $\tilde{E}_{\mathrm{xc}}^{\mathrm{DFT}}$ is given by[11]

$$\tilde{E}_{\mathrm{xc}}^{\mathrm{DFT}} = (1 - a_0)E_{\mathrm{x}}^{\mathrm{DFT}} + E_{\mathrm{DC}}^{\mathrm{DFT}} \tag{3}$$

where $E_{\mathrm{x}}^{\mathrm{DFT}}$ stands for the LSDA, GGA, or meta-GGA exchange energy and $E_{\mathrm{DC}}^{\mathrm{DFT}}$ simulates dynamical (short-range) correlation within one of these approximations ($E_{\mathrm{DC}}^{\mathrm{DFT}}$ is often termed just "correlation energy" and denoted as $E_{\mathrm{c}}^{\mathrm{DFT}}$). An important reason for the success of hybrid functionals is that they provide a balance between a reduction of the Coulomb self-interaction error (SIE) and the simulation of nondynamical correlation (NDC).[12–14] The exact exchange (EXX) energy (eq 2) is free from SIE, while the DFT exchange $\tilde{E}_{\mathrm{x}}^{\mathrm{DFT}}$ accounts implicitly for some NDC due to the local character of its exchange hole.[15] For traditional ("global") hybrids, this balance is determined by the constant amount of the EXX admixture, a_0 (eq 1).[16] Increased attention has recently been given to the limits in the achievable accuracy and universality of this ansatz. It is usually not possible to find a unique value of a_0 to obtain optimum accuracy for a wide range of properties or for different types of molecular or solid-state systems. For example, with GGA approximations for $\tilde{E}_{\mathrm{xc}}^{\mathrm{DFT}}$, the best performance for thermochemical properties (in particular, for atomization energies) requires rather modest EXX admixtures of typically about 0.16−0.30 (some theoretical justifications have been put forward[17]), whereas larger values tend to be optimum for, e.g., reaction barriers[18] or for some linear response properties.[19]

In the past decade, the concept of hybrid functionals has been generalized into two different, promising directions. One of them has led to the notion of "range-separated hybrid functionals", where the electron-electron repulsion energy is split into short-range and long-range contributions along the interelectronic coordinate.[20] The second route, considered in the present work, is the so-called local hybrid functionals.[12–14,21–26] Here, the EXX admixture is not a constant but a function of coordinates in real space (a local mixing function, LMF)[13]

$$E_{\mathrm{xc}}^{\mathrm{loc\text{-}hyb}} = \sum_{\sigma=\alpha,\beta}\int \{g_\sigma(\mathbf{r})\varepsilon_{\mathrm{x},\sigma}^{\mathrm{exact}}(\mathbf{r}) + [1 - g_\sigma(\mathbf{r})]\varepsilon_{\mathrm{x},\sigma}^{\mathrm{DFT}}(\mathbf{r})\}\mathrm{d}\mathbf{r} + E_{\mathrm{c}}^{\mathrm{DFT}} \tag{4}$$

that is, constant a_0 (eqs 1 and 3) is replaced by the LMF $g_\sigma(\mathbf{r})$. One usually assumes that

---

† Part of the "Walter Thiel Festschrift".

* To whom correspondence should be addressed. Fax: +49-931-888-71-35. E-mail: arbouznikov@mail.uni-wuerzburg.de (A.V.A.); kaupp@mail.uni-wuerzburg.de (M.K.).

10.1021/jp903233q CCC: $40.75

$$0 \le g(\mathbf{r}) \le 1 \tag{5}$$

In contrast to the integrated energies E_x^{exact} and E_x^{DFT} in eqs 1 and 3, the corresponding local energy densities $\varepsilon_{x,\sigma}^{\text{exact}}$ and $\varepsilon_{x,\sigma}^{\text{DFT}}$ ($\sigma = \alpha, \beta$) enter eq 4. By definition

$$E_x^{\text{DFT}} = \sum_{\sigma=\alpha,\beta} E_{x,\sigma}^{\text{DFT}} = \sum_{\sigma=\alpha,\beta} \int \varepsilon_{x,\sigma}^{\text{DFT}}(\mathbf{r})\mathrm{d}\mathbf{r} \tag{6}$$

and

$$E_x^{\text{exact}} = \sum_{\sigma=\alpha,\beta} E_{x,\sigma}^{\text{exact}} = \sum_{\sigma=\alpha,\beta} \int \varepsilon_{x,\sigma}^{\text{exact}}(\mathbf{r})\mathrm{d}\mathbf{r} \tag{7}$$

We note that energy densities (unlike integrated energies) are "gauge-dependent" and hence not unique quantities. They may be calibrated arbitrarily by adding some function which integrates to 0.[27,28] It is easy to show that any mismatch in the gauge origin of mixed energy densities creates an error that hampers refinement of LMFs (i.e., it is not straightforward to eliminate such errors just by a special choice of the LMF). The effect of the gauge dependence of the exchange energy densities on the quality of a resulting local hybrid is currently not fully clear but is suggested to be moderate by some recent studies.[26,29,30] For reasons addressed further below, we will employ the conventional gauge for both the EXX energy density

$$\varepsilon_{x,\sigma}^{\text{exact}}(\mathbf{r}) = -\frac{1}{2}\sum_{i_\sigma j_\sigma}^{\text{occ}} \varphi_{i_\sigma}^{*}(\mathbf{r})\varphi_{j_\sigma}(\mathbf{r}) \int \frac{\varphi_{j_\sigma}^{*}(\mathbf{r}')\varphi_{i_\sigma}(\mathbf{r}')}{|\mathbf{r}-\mathbf{r}'|}\mathrm{d}\mathbf{r}' \qquad \sigma = \alpha,\beta \tag{8}$$

and the LSDA exchange energy density

$$\varepsilon_{x,\sigma}^{\text{LSDA}}(\mathbf{r}) = -\frac{3}{2}\left(\frac{3}{4\pi}\right)^{1/3}\rho_\sigma^{4/3}(\mathbf{r}) \qquad \sigma = \alpha,\beta \tag{9}$$

(other types of exchange energy densities will only be mentioned in passing).

By their very construction, local hybrids are clearly more flexible than standard global hybrids, and they should thus be able to provide an improved balance between the reduction of SIE and the simulation of NDC. Indeed, some recent results with rather simple one-parameter LMFs have provided numerical evidence for this point by exhibiting simultaneously accurate atomization energies (which depend decisively on the simulation of left-right correlation in bonding) and reaction barriers (which require often a reduction of NDC at the transition state and are affected significantly by SIE),[14] as well as response properties (in particular, nuclear shielding constants[31]). These data have already pointed to improved universality of local versus global hybrids. The performance of local hybrids is determined by (i) the choice of the LMF, that is, the spatial dependence of the mixture and (ii) the nature of the $\tilde{E}_{xc}^{\text{DFT}}$ used. So far, the clearly best results for computational thermochemistry and kinetics, with dramatic improvement over the underlying global hybrid, have been obtained[14,22] when mixing just LSDA exchange ("Slater exchange",[4] without GGA or meta-GGA contributions) with exact exchange, using the simple one-parameter LMF (a scaled variant of a previously suggested LMF[13])

$$g_\sigma(\mathbf{r}) = 0.48 t_\sigma(\mathbf{r}) \tag{10}$$

$$t_\sigma(\mathbf{r}) = \frac{\tau_{W,\sigma}(\mathbf{r})}{\tau_\sigma(\mathbf{r})} \tag{11}$$

Here, $\tau_\sigma(\mathbf{r})$ is the σ-spin local kinetic energy density

$$\tau_\sigma(\mathbf{r}) = \frac{1}{2}\sum_{i_\sigma}^{\text{occ}} |\nabla\varphi_{i_\sigma}(\mathbf{r})|^2 \tag{12}$$

and $\tau_{W,\sigma}(\mathbf{r})$ is the corresponding von Weizsäcker kinetic energy density

$$\tau_{W,\sigma}(\mathbf{r}) = \frac{1}{8}\frac{|\nabla\rho_\sigma(\mathbf{r})|^2}{\rho_\sigma(\mathbf{r})} \tag{13}$$

The VWN LSDA[6] has been used for dynamical correlation, and the resulting local hybrid has been denoted as "*Lh*-SVWN", with explicit indication of the LMF.[14,22]

Other types of LMFs examined so far include (i) functions depending on the dimensionless density gradient,[14,23] $g(\mathbf{r}) = F[s_\sigma(\mathbf{r})]$, where

$$s_\sigma(\mathbf{r}) = \frac{|\nabla\rho_\sigma(\mathbf{r})|}{2(3\pi^2)^{1/3}\rho_\sigma^{4/3}(\mathbf{r})} \approx \frac{|\nabla\rho_\sigma(\mathbf{r})|}{6.1873\rho_\sigma^{4/3}(\mathbf{r})} \qquad \sigma = \alpha,\beta \tag{14}$$

and F is a monotonous mapping of the semi-infinite interval $[0; \infty]$ onto the finite $[0; 1]$; (ii) constructions based on density matrix similarity metrics;[24] and (iii) more sophisticated functions including energy densities, designed to satisfy as many exact physical constraints as possible.[26] We have also examined the construction of LMFs in a purely ab initio framework based on a local version of the adiabatic connection formalism.[25] So far, together with the very complicated five-parameter functional of ref 26, the "semi-empirical" LMFs based on physically intuitive inhomogeneity parameters like $t_\sigma(\mathbf{r})$ or $s_\sigma(\mathbf{r})$ (in the following denoted as *t*-LMFs and *s*-LMFs, respectively) have provided the best numerical results[14,22,23] and thus apparently the best SIE/NDC balance for the properties and systems examined. Here, we extend and further improve these types of LMFs by introducing spin polarization as an additional variable. The resulting two-parameter LMFs are then optimized for small calibration sets of atomization energies and reaction barriers and subsequently evaluated for more extended test sets.

II. Theory

A. Local Hybrids versus Models for Nondynamical Correlation. Our introduction of spin polarization into LMFs for local hybrids (see below) has been stimulated by a different, recently proposed way to include NDC into exchange–correlation functionals, that is, Becke's coordinate space model of nondynamical correlation (B05).[32,33] This approach starts from 100% EXX and compensates the too-delocalized nature of the EXX hole in certain situations (e.g., upon bond stretching) by an appropriately nonlocal NDC hole. The total B05 exchange-correlation functional is written as

$$E_{\mathrm{xc}}^{\mathrm{B05}} = E_{\mathrm{x}}^{\mathrm{exact}} + a_{\mathrm{NDC}}^{\mathrm{opp}}E_{\mathrm{NDC}}^{\mathrm{opp}} + a_{\mathrm{NDC}}^{\mathrm{par}}E_{\mathrm{NDC}}^{\mathrm{par}} + E_{\mathrm{DC}} \tag{15}$$

where $E_{\mathrm{NDC}}^{\mathrm{opp}}$ and $E_{\mathrm{NDC}}^{\mathrm{par}}$ stand for the nondynamical correlation between opposite spin and parallel spin electrons, respectively, and $a_{\mathrm{NDC}}^{\mathrm{opp}}$ and $a_{\mathrm{NDC}}^{\mathrm{par}}$ are fitting coefficients (positive numbers not much less than 1). While we have recently examined in detail the problems arising in the self-consistent implementation of the full B05 model for open-shell cases,[34] here we are interested only in the general structure of the underlying equations. The predominant NDC energy contribution arises from the interactions between opposite spin electrons and is (unscaled)

$$E_{\mathrm{NDC}}^{\mathrm{opp}} = \int f(\mathbf{r})\frac{\rho_\alpha(\mathbf{r})}{\rho_\beta(\mathbf{r})}\varepsilon_{\mathrm{x},\beta}^{\mathrm{exact}}(\mathbf{r})\mathrm{d}\mathbf{r} + \int f(\mathbf{r})\frac{\rho_\beta(\mathbf{r})}{\rho_\alpha(\mathbf{r})}\varepsilon_{\mathrm{x},\alpha}^{\mathrm{exact}}(\mathbf{r})\mathrm{d}\mathbf{r} \tag{16}$$

where $f(\mathbf{r})$ is a sophisticated, highly nonlinear (implicitly defined and nonsmooth) function of both alpha and beta spin densities, their gradients, Laplacians, noninteracing kinetic energy densities (eq 12), and, finally, the EXX energy density (eq 8).[35] The smaller but still important parallel spin NDC energy is given by

$$E_{\mathrm{NDC}}^{\mathrm{par}} = E_{\mathrm{NDC}}^{\alpha\alpha} + E_{\mathrm{NDC}}^{\beta\beta} \tag{17}$$

where

$$E_{\mathrm{NDC}}^{\sigma\sigma} = \int \rho_\sigma(\mathbf{r})B_\sigma(\mathbf{r})\mathrm{d}\mathbf{r} \qquad \sigma = \alpha, \beta \tag{18}$$

and function $B_\sigma(\mathbf{r})$ is determined mainly by σ-spin quantities (i.e., the dependence on σ'-spin quantities, $\sigma' \neq \sigma$, is weaker).[36] The expression for $E_{\mathrm{NDC}}^{\sigma\sigma}$ ($\sigma = \alpha, \beta$) resembles structurally $E_{\mathrm{NDC}}^{\mathrm{opp}}$, except that further, even more complicated functions are employed in the corresponding integrand (see refs 32 and 33 for details).

To draw analogies between local hybrids and the B05 model and following ref 26, we may formally rewrite eq 4 for local hybrids as

$$\begin{aligned} E_{\mathrm{xc}}^{\text{loc-hyb}} &= E_{\mathrm{x}}^{\mathrm{exact}} + \sum_{\sigma=\alpha,\beta}\int[1 - g_\sigma(\mathbf{r})][\varepsilon_{\mathrm{x},\sigma}^{\mathrm{DFT}}(\mathbf{r}) - \varepsilon_{\mathrm{x},\sigma}^{\mathrm{exact}}(\mathbf{r})]\mathrm{d}\mathbf{r} + E_{\mathrm{DC}} \\ &= E_{\mathrm{x}}^{\mathrm{exact}} + E_{\mathrm{NDC}}^{\text{loc-hyb}} + E_{\mathrm{DC}} \end{aligned} \tag{19}$$

with

$$E_{\mathrm{NDC}}^{\text{loc-hyb}} = E_{\mathrm{NDC},\alpha}^{\text{loc-hyb}} + E_{\mathrm{NDC},\beta}^{\text{loc-hyb}} \tag{20a}$$

and

$$E_{\mathrm{NDC},\sigma}^{\text{loc-hyb}} = \int[1 - g_\sigma(\mathbf{r})][\varepsilon_{\mathrm{x},\sigma}^{\mathrm{DFT}}(\mathbf{r}) - \varepsilon_{\mathrm{x},\sigma}^{\mathrm{exact}}(\mathbf{r})]\mathrm{d}\mathbf{r} \qquad \sigma = \alpha, \beta \tag{20b}$$

As the LMF $g_\sigma(\mathbf{r})$ is involved exclusively in the term $E_{\mathrm{NDC}}^{\text{loc-hyb}}$, we will, for brevity, sometimes call this term loosely "local hybrid" in the following. Comparison of $E_{\mathrm{NDC}}^{\text{loc-hyb}}$ (eq 20) with $E_{\mathrm{NDC}}^{\mathrm{B05}} = a_{\mathrm{NDC}}^{\mathrm{opp}}\ E_{\mathrm{NDC}}^{\mathrm{opp}} + a_{\mathrm{NDC}}^{\mathrm{par}}\ E_{\mathrm{NDC}}^{\mathrm{par}}$ (eqs 15−18) indicates the former to be clearly structurally simpler. In particular, in the integrand on the right-hand side (RHS) of eq 20b, all analytical forms of g_σ known up to now (except one[26]) are determined by same-spin ("σ-spin") quantities only and do not depend on opposite spin ingredients. It may seem paradoxical, but it is the basic structure of a hybrid functional that opposite spin NDC is mimicked by information on the same-spin subsystem only and that eqs 19 and 20 lack "cross terms" (or "other spin terms") like those occurring in eq 16. Obviously, these differences between the two constructions vanish for closed-shell systems (see discussion below).

In the following, we will not attempt to fully mimic or approximate the B05 functional by local hybrids but only incorporate an important structural feature of the former into our LMFs. The simplest way to introduce such cross terms in an ad hoc fashion would be to interchange the LMF-dependent factors between alpha and beta spin terms in eq 20

$$E_{\mathrm{NDC},\sigma}^{\text{loc-hyb}} = \int[1 - g_\sigma(\mathbf{r})][\varepsilon_{\mathrm{x},\sigma'}^{\mathrm{DFT}}(\mathbf{r}) - \varepsilon_{\mathrm{x},\sigma'}^{\mathrm{exact}}(\mathbf{r})]\mathrm{d}\mathbf{r} \qquad \sigma = \alpha, \beta, \sigma' \neq \sigma \tag{21}$$

In local hybrid eq 21, the LMF determined by alpha spin quantities controls the beta spin EXX admixture and vice versa. However, we decided to choose a less drastic approach, as detailed in the following.

B. Spin Polarization As an Additional Variable of Local Mixing Functions. Another way to introduce the above-mentioned opposite spin terms into local hybrids is by using the spin polarization ζ as an additional variable

$$\zeta(\mathbf{r}) = \frac{\rho_\alpha(\mathbf{r}) - \rho_\beta(\mathbf{r})}{\rho(\mathbf{r})} \qquad \text{where} \quad \rho(\mathbf{r}) = \rho_\alpha(\mathbf{r}) + \rho_\beta(\mathbf{r}) \tag{22}$$

The inclusion of spin polarization is also useful from other viewpoints (see below). Note that $-1 \le \zeta \le 1$, but overall, ζ is predominantly positive (except for strongly spin-contaminated SCF solutions). For brevity, hereafter, we omit the argument $\mathbf{r}$ where the latter is immaterial. We emphasize that ζ is employed here in a completely different context than in a recent local hybrid of Perdew and co-workers.[26]

Using ζ, we modify the best previous *t*- and *s*-LMFs[14,22,23] and obtain two *t*-ζ- and *s*-ζ-LMFs (eqs 23 and 24, respectively)

$$g_\alpha = (b + c\zeta)t_\alpha \tag{23a}$$

$$g_\beta = (b - c\zeta)t_\beta \tag{23b}$$

$$g_\alpha = \mathrm{erf}[(b + c\zeta)s_\alpha] \tag{24a}$$

$$g_\beta = \mathrm{erf}[(b - c\zeta)s_\beta] \tag{24b}$$

The variables t_σ and s_σ are given by eqs 11 and 14, respectively. At first glance, the analytical form of the LMFs (eqs 23 and 24) looks somewhat restrictive, and one might wonder about using a more flexible ansatz like, for example

$$g_\alpha = F[(b_\alpha + c_\alpha\zeta)t_\alpha] \text{ or } F[(b_\alpha + c_\alpha\zeta)s_\alpha] \quad (25a)$$

and

$$g_\beta = F[(b_\beta + c_\beta\zeta)t_\beta] \text{ or } F[(b_\beta + c_\beta\zeta)s_\beta] \quad (25b)$$

with independent values of b_α, c_α, b_β, and c_β (the particular form of F in eq 25 is unimportant). Indeed, for non-selfconsistent (post-Hartree-Fock, post-LDA, post-GGA, etc.) calculations of total energies, any unconstrained b_σ and c_σ ($\sigma = \alpha, \beta$) could be used, and even a "generalization" of eq 10

$$g_\sigma = b_\sigma t_\sigma \qquad \sigma = \alpha, \beta \quad (26)$$

with $b_\alpha \neq b_\beta$, could be envisioned. However, evaluation of functional derivatives of the corresponding energy functional (eq 19) with respect to the occupied orbitals, $\delta E^{\text{loc-hyb}}_{\text{NDC},\sigma}/\delta\varphi_{i,\sigma}$, needed for self-consistent implementation, must respect the constraints

$$b_\beta = b_\alpha \quad (27a)$$

and

$$c_\beta = -c_\alpha \quad (27b)$$

Otherwise closed-shell systems will exhibit spurious spin polarization during the SCF (see Appendix).

There is no straightforward way to identify "opposite spin NDC" and "parallel spin NDC" in the functional defined by eq 20 if the corresponding LMF is a nonlinear function of ζ, t_σ, and/or s_σ [like, e.g., in eqs. 24]. Such a separation may be done for the particular case of a linear function given by eqs. 23. Then, eqs 20 may be rewritten as

$$E^{\text{loc-hyb}}_{\text{NDC}} = E^{\text{loc-hyb}}_{\text{NDC,opp}} + \sum_{\sigma=\alpha,\beta} E^{\text{loc-hyb}}_{\text{NDC,par},\sigma} \quad (28)$$

where

$$E^{\text{loc-hyb}}_{\text{NDC,par},\sigma}(\mathbf{r}) = \int \left\{1 - \left[b + \frac{c\rho_\sigma(\mathbf{r})}{\rho(\mathbf{r})}\right]t_\sigma(\mathbf{r})\right\} \times [\varepsilon^{\text{DFT}}_{\text{x},\sigma}(\mathbf{r}) - \varepsilon^{\text{exact}}_{\text{x},\sigma}(\mathbf{r})]\text{d}\mathbf{r} \quad (29)$$

and

$$E^{\text{loc-hyb}}_{\text{NDC,opp}}(\mathbf{r}) = c\int \sum_{\sigma=\alpha,\beta} \frac{\rho_{\sigma'}(\mathbf{r})}{\rho(\mathbf{r})} t_\sigma(\mathbf{r})[\varepsilon^{\text{DFT}}_{\text{x},\sigma}(\mathbf{r}) - \varepsilon^{\text{exact}}_{\text{x},\sigma}(\mathbf{r})]\text{d}\mathbf{r} \qquad \sigma' \neq \sigma \quad (30)$$

A basic qualitative difference between such local hybrids and the B05 NDC model remains; as will be shown below, efficient local hybrids with t-ζ-LMFs (eq 23) obtain optimized values on the order of $b = 0.4$ and $c = 0.05$. Then, eqs 29 and 30 mean clearly $|E^{\text{loc-hyb}}_{\text{NDC,opp}}| < |E^{\text{loc-hyb}}_{\text{NDC,par}}|$, whereas the opposite relation between the two NDC contributions is expected.[32,33] However, both in explicit NDC models like B05[32,33] and in the present model, each of the spin components of the parallel spin NDC energies depends always on other-spin quantities. This speaks against overrating separations like those in eqs 28−30. Strictly speaking, there is no complete separation of alpha and beta spin variables in eqs 29 and 30, as both expressions contain $\rho = \rho_\alpha + \rho_\beta$.

C. Notes on the Choice of Gauge for Energy Densities. Here, we provide a partial rationalization of the previously observed particularly good performance of local hybrids that mix only LSDA exchange and EXX without GGA contributions.[14,22,23] As mentioned above, the nonuniqueness of energy densities is an underlying fundamental potential problem of any functional relying on these quantities.[27,28] For local hybrids (eq 4), both DFT exchange and EXX energy densities should be represented in the same gauge. Otherwise, a spurious residue arises that may affect the performance of the functional and is hard or impossible to eliminate (see Introduction). In two recent studies,[26,29] the EXX energy density gauge has been adjusted approximately to that of the GGA or meta-GGA exchange energy density by adding a calibration function. However, the opposite way may be chosen as well: starting from the conventional definition of the EXX energy density (eq 8), consider its gauge as the reference, and try to adjust the DFT exchange energy density to this gauge. While a rigorous adjustment is certainly nontrivial for GGA or meta-GGA exchange, the LSDA exchange energy density (eq 8) appears to be close to the EXX reference gauge by definition. For the homogeneous limit, this may be shown via the well-known derivations of eq 9, starting from exact exchange (eqs 7 and 8) followed by substitution by plane waves for a particle in a box (which describe one-particle states in the uniform electron gas) in place of orbitals φ_i. Integration over only one set of three-dimensional variables, say $\mathbf{r}'$, and some transformations typical for uniform electron gas theory leads to eq 9 (see chapter 6.1 of ref 37 for details). That is, LSDA and EXX gauges for exchange energy densities are identical in the homogeneous limit by definition. While this is of course also true for GGA or meta-GGA functionals (which reduce to the LSDA in the homogeneous limit), in those cases, the enhancement factors involve partial integrations of the underlying exchange energy densities or exchange holes, which are usually performed to remove higher derivatives of the electron density (see, e.g., refs 2b and 8). Most likely, these enhancement factors introduce a larger deviation of the GGA and meta-GGA gauge from that of the exact exchange energy density than is the case for the simple and straightforward LSDA energy density (cf. eq 9). This may explain the surprisingly good performance of local hybrids based on LSDA and exact exchange only. For future work, one may envision the a priori construction of new GGA or meta-GGA enhancement factors with improved gauge, specifically for the use in local hybrids.

What seems less straightforward to understand at first sight is the observation that, so far, local hybrids with LSDA (VWN) dynamical correlation have performed best.[14,22,23] This may have to do with a good match between LSDA exchange and correlation contributions; in regions without or with low exact exchange admixtures, LSDA exchange dominates but is known to underestimate exact exchange. This is partly compensated for by the too large LSDA correlation.[15] Other possible implicit error cancellations at work in local hybrids still remain to be analyzed.

III. Computational Details

We report here results obtained with *Lh*-SVWN functionals (see above), where the LMFs have been chosen according to

TABLE 1: Optimized Parameters of Local Mixing Functions and Results for the Fit Set of Atomization Energies and Reaction Barriers (in kcal mol^{-1})[a]

		AE6		BH6	
Functional	LMF	MAE	MSE	MAE	MSE
B3LYP		3.91	−3.07	4.81	−4.81
Lh-SVWN	$g_\sigma = 0.48 t_\sigma$ ($\sigma = \alpha, \beta$)	3.45	1.52	2.78	−2.23
Lh-SVWN	$g_\alpha = (0.446 + 0.0531\zeta) t_\alpha$ $g_\beta = (0.446 - 0.0531\zeta) t_\beta$	1.73	0.53	3.07	−3.07
Lh-SVWN	$g_\sigma = \mathrm{erf}(0.22 s_\sigma)$ ($\sigma = \alpha, \beta$)	5.2	1.81	3.80	−3.80
Lh-SVWN	$g_\alpha = \mathrm{erf}[(0.197 + 0.0423\zeta) s_\alpha]$ $g_\beta = \mathrm{erf}[(0.197 - 0.0423\zeta) s_\beta]$	2.53	0.50	4.64	−4.64

[a] *Lh*-SVWN local hybrids, results with an uncontracted QZVP basis. The fit set[44] contains six atomization energies (AE6) and six barrier heights (BH6). For comparison, results with B3LYP and previously reported local hybrids without dependence on ζ are also shown. See eqs 11 and 14 for the definitions of t_σ and s_σ, respectively.

eqs 23 and 24. While our earlier studies of local hybrids[14,22,23,25] were based on the MAG-ReSpect code,[38] all of the calculations reported in this paper have been performed using a locally modified version of the Turbomole package.[39] Other changes in the computational details include (i) replacement of a truncated cc-pVQZ basis set[40] (*g* functions were omitted in the past) to the fully uncontracted QZVP[41] basis set;[42] (ii) non-self-consistent evaluation of total energies using B3LYP orbitals rather than those obtained previously with 10% exact exchange mixed with Slater exchange and VWN correlation;[43] (iii) the semiempirical parameters entering the LMF being optimized for the small AE6 and BH6 sets consisting of six atomization energies (AEs) and six barrier heights (BHs)[44,45] (instead of previous optimizations that were done for the G2-1 test set of 55 atomization energies[46]). A completeness insertion in the uncontracted orbital basis set has been used to compute the exact exchange energy density in eq 8.[42,47]

We will also give results obtained with previously reported functionals.[14,22,23] This allows the effect of the changes to be seen (as in our previous studies, we use MP2-optimized structures for the full G2[48] and G3 sets;[49] this leads to somewhat larger mean absolute errors than those found for B3LYP-optimized structures that have been used in some evaluations in the literature[50]). The HTBH38/04[51] and NHTBH38[52] compilations of classical barriers for hydrogen and heavier-atom transfer reactions, respectively, have been employed in our validation studies of the performance of new local hybrids for "computational kinetics". Dissociation energies for two-center three-electron dimer cations X_2^+ refer generally to the correct asymptote $X + X^+$.

IV. Results and Discussion

Fitting of the two free parameters *b* and *c* of the *t*-ζ- and *s*-ζ-LMFs (eqs 23 and 24) against the AE6 set of six atomization energies and the BH6 set of six reaction barriers (with a 1:1 weighting) leads to the results shown in Table 1. Data for the original *t*- and *s*-LMFs, which may be described by the same equations with *c* set to 0, are also given. Introduction of the $c\zeta$ term clearly improves the atomization energies but deteriorates the barriers slightly. The optimized values of the additional parameter *c* are about one order of magnitude smaller than the leading parameter *b* in both the *t*-ζ- and *s*-ζ-LMFs. Parameter *b* is decreased by about 7−10% compared to its original value in the former *t*- and *s*-LMFs (Table 1). This reduces the overall exact exchange admixture in the functional for closed-shell systems ($\zeta = 0$) and explains why the barriers tend to be reduced and thereby deteriorated somewhat. We note in passing that one could of course prefer a lower weighting of the AE6 atomization energies relative to the BH6 barriers (other than the 1:1 weighting used). This provides slightly worse atomization energies but better barriers. Apparently, these two-parameter LMFs are not yet sufficiently flexible to allow a completely independent optimization of both barriers and atomization energies. Parameter *c* is in both cases positive. That is, it adds some exact exchange for the alpha spin subsystem of the open-shell species while reducing it for the beta spin manifold.

Table 2 evaluates the thermochemical performance for the larger G3 test set. We first note that for the one-parameter functionals without ζ dependence, the somewhat different computational procedure changes the mean signed and absolute errors somewhat compared to our earlier calculations,[14] but not decisively. Upon inclusion of spin polarization, we see the same behavior as that suggested by the small AE6 set results above: the *t*-ζ- and *s*-ζ-LMFs perform appreciably better than their unpolarized counterparts. The improvement is particularly notable for the *s*-ζ-LMF, where the mean absolute error for the full G3 set has dropped by 40%. However, even for the *t*-ζ-LMF, the MAE is reduced by about 1 kcal mol^{-1}. Given their very simple structure with only LSDA exchange and correlation and exact exchange and only two adjustable parameters, both the *t*-ζ and *s*-ζ local hybrids provide G3 set atomization energies that are a remarkable improvement over standard functionals like B3LYP (Table 2). To our knowledge, the obtained mean absolute errors near 3.0 kcal mol^{-1} (given the MP2-optimized structures; cf. Computational Details) are competitive with any known occupied-orbital-dependent functional (and close to "double hybrids" like B2PLYP, which incorporate electron correlation via inclusion of the virtual orbital space in a MP2-like correlation term[53]). A further notable observation is that, while the original *s*-LMF exhibits an increase of the MAE when extending the test set from G2-1 to G3 (albeit much less than B3LYP), in the case of the *s*-ζ-LMF, the error even decreases slightly.

The ζ-dependence makes an effect exclusively for open-shell systems. While the small G2-1 test set includes 18 open-shell species out of 55 molecules (~1/3), this number drops to 12 for the remainder of the G2 set (totally, 93 molecules and radicals) and becomes very small (only 2) for the subset of 75 species constituting the rest of the full G3 set. Yet, the improvement of the atomization energies by inclusion of the ζ dependence is notable for all of the subsets. This points to an improvement predominantly of the reference valence atomic energies (13 of 14 atoms involved in the G3 test set are open-shell species). Note that here, we specifically do not refer to the quality of the total energies as these are appreciably affected by the LMF in the core region, which we have not attempted to optimize so far.

As could already be inferred from the small calibration sets above (Table 1), the significantly improved thermochemical performance of the "spin-polarized" LMFs is accompanied by a moderate deterioration of the barriers. Table 3 shows that in both the *s*-LMF and *t*-LMF cases, the MAE for the non-hydrogen-transfer barriers (NHTBH38/04) remains essentially unchanged (0.1 kcal mol^{-1} increase), whereas that of the hydrogen-transfer barriers (HTBH38/04) increases by about 0.8 kcal mol^{-1}. This reflects the very slightly lower overall exact exchange admixture.

TABLE 2: Mean Absolute and Signed Errors (in kcal mol^{-1}) in the Atomization Energies of the G3 Test Set and Subsets[a]

		G2-1 (55)		G2 (93)		G3 (75)		ΣG3 (223)	
functional	LMF	MAE	MSE	MAE	MSE	MAE	MSE	MAE	MSE
B3LYP		2.53	−0.35	4.61	−4.10	10.76	−10.73	6.17	−5.41
Lh-SVWN	$g_\sigma = 0.48t_\sigma$ ($\sigma = \alpha, \beta$)	3.73	0.98	4.35	1.53	3.31	−0.12	3.85	0.84
Lh-SVWN	$g_\alpha = (0.446 + 0.0531\zeta)t_\alpha$ $g_\beta = (0.446 - 0.0531\zeta)t_\beta$	2.66	0.20	2.97	1.43	3.16	−0.58	2.96	0.45
Lh-SVWN	$g_\sigma = \mathrm{erf}(0.22s_\sigma)$ ($\sigma = \alpha, \beta$)	4.91	1.66	5.51	2.12	5.22	0.00	5.26	1.30
Lh-SVWN	$g_\alpha = \mathrm{erf}[(0.197 + 0.0423\zeta)s_\alpha]$ $g_\beta = \mathrm{erf}[(0.197 - 0.0423\zeta)s_\beta]$	3.30	0.60	3.21	1.74	2.97	−1.23	3.15	0.46

[a] Results with an uncontracted QZVP basis. The data with the "non-spin-polarized" LMFs differ very slightly from our previous results[14] obtained with slightly different computational settings (truncated cc-pVQZ basis set, SVWN-10 orbitals, ReSpect program; see Computational Details).

TABLE 3: Mean Absolute and Signed Errors (in kcal mol^{-1}) for Classical Barrier Heights[a]

		HTBH38/04		NHTBH38/04	
functional	LMF	MAE	MSE	MAE	MSE
B3LYP		4.3	−4.3	5.0	−4.8
Lh-SVWN	$g_\sigma = 0.48t_\sigma$ ($\sigma = \alpha, \beta$)	2.5	−2.1	2.5	−1.5
Lh-SVWN	$g_\alpha = (0.446 + 0.0531\zeta)t_\alpha$ $g_\beta = (0.446 - 0.0531\zeta)t_\beta$	3.30	−2.90	2.60	−1.90
Lh-SVWN	$g_\sigma = \mathrm{erf}(0.22s_\sigma)$ ($\sigma = \alpha, \beta$)	3.5	−3.4	4.3	−3.7
Lh-SVWN	$g_\alpha = \mathrm{erf}[(0.197 + 0.0423\zeta)s_\alpha]$ $g_\beta = \mathrm{erf}[(0.197 - 0.0423\zeta)s_\beta]$	4.3	−4.3	4.4	−4.4

[a] Results with an uncontracted QZVP basis. The data with the "non-spin-polarized" LMFs differ very slightly from our previous results[14] obtained with slightly different computational settings (truncated cc-pVQZ basis set, SVWN-10 orbitals, ReSpect program; see Computational Details).

So far, the description of two-center three-electron dimer cations like those shown in Table 4 has remained a challenge for all functionals as their accurate description by DFT requires a large amount of exact exchange (NDC is unimportant for bonding in these systems, but SIE is a serious problem[54,55]) that is incompatible with good general thermochemical performance. Unfortunately, this problem is not cured by the local hybrids based on the spin-polarized LMFs (Table 4; CCSD(T) results[55,56] are used as reference data). All local hybrids under consideration give significant overbinding and too large equilibrium bond lengths and are only somewhat better than B3LYP. The spin-polarized LMFs give essentially the same distances as their unpolarized counterparts and marginally larger binding energies (likely due to the overall somewhat lower exact exchange, given the slightly lower parameter *b*). Apparently, the flexibility of the present one- and two-parameter local hybrids is not sufficient to extend the good performance for general thermochemical and barrier data to these systems with rather special bonding situations.

As we have reported earlier (cf. ref 23 and references therein), an interesting relationship is observed for the local hybrids with both *t*- and *s*-LMFs when comparing density-averaged local mixing functions

$$\bar{g}_\sigma = \int g_\sigma(\mathbf{r})\rho_\sigma(\mathbf{r})d\mathbf{r} \Big/ \int \rho_\sigma(\mathbf{r})d\mathbf{r} = (1/N_\sigma)\int g_\sigma(\mathbf{r})\rho_\sigma(\mathbf{r})d\mathbf{r} \qquad \sigma = \alpha, \beta \qquad (31)$$

For almost all open-shell systems studied, we observe

$$\bar{g}_\beta > \bar{g}_\alpha \text{ or } \Delta\bar{g} \equiv \bar{g}_\beta - \bar{g}_\alpha > 0 \qquad (32)$$

in spin-unrestricted calculations. In other words, the averaged minority spin LMF is almost always larger than the averaged majority spin LMF. Therefore, as was mentioned above, one might expect from Table 1 and eqs 23 and 24 that the difference, $\Delta\bar{g}$ in eq 32, will be reduced upon inclusion of the explicit dependence on ζ. This is indeed the case, as one can see from Table 5. Apparently, the decrease of $\Delta\bar{g}$ is significantly larger than one could expect only from the reduction of factor *b* (eqs 23 and 24). This effect is particularly pronounced for *s*-ζ-LMFs, where $\Delta\bar{g}$ drops by more than a factor of 2 on average. This "damping" of the differences between the density-averaged α- and β-spin LMFs correlates with the observed improved thermochemical performance. The reasons for this correlation remain to be studied in more detail.

An advantage of the *s*-LMFs (e.g., eq 24) over the scaled *t*-LMFs (eqs 10 and 23) is the correct long-range behavior (i.e., *g* goes to 1 as the density goes to 0). Yet, the overall performance of the scaled *t*-LMFs for thermochemistry and barriers is better (see above). Figure 1 shows that we can easily restore the correct long-range behavior of a scaled *t*-LMF by adding a suitable *s*-LMF contribution. The example two-parameter LMF shown (dashed line) provides identical atomization energies and barriers as the original *t*-LMF (solid line; eq 10). We have so far not attempted to optimize the parameters of such "mixed" LMFs (or of three-parameter LMFs that also include ζ), as this requires an implementation and optimization of properties (e.g., charge-transfer excitation energies in time-dependent DFT calculations) that depend crucially on the long-range part of the functional. This is ongoing work.

V. Conclusions and Outlook

Introduction of spin polarization as an explicit variable into the local mixing functions (LMFs) that determine the position-dependent mixture of local and exact exchange in local hybrid functionals is motivated by considerations of implicit and explicit treatments of nondynamical correlation (NDC) in DFT. The resulting two-parameter LMFs suggested here and the LSDA-based local hybrids based thereon provide remarkable state-of-the-art accuracy for thermochemistry, with significant improvement over previously suggested one-parameter LMFs. At the same time, the accuracy for classical activation barriers is deteriorated only moderately. Yet, the optimization results indicate that these two-parameter functionals are not yet flexible enough to optimize barriers and thermochemistry simultaneously. Cases like two-center three-electron dimer cations, in which NDC is essentially absent but where self-interaction errors are particularly severe, are not yet improved sufficiently. The current LMFs eliminate self-interaction errors fully only at long range (see above), and it will be necessary to extend the correct behavior to a larger relevant part of the electron density

TABLE 4: Dissociation Energies (in kcal mol^{-1}) and Equilibrium Bond Lengths (in Å) of Two-Center Three-Electron Dimer Cations[a]

LMF		H_2^+		He_2^+		Ne_2^+		Ar_2^+		$(HF)_2^+$		$(H_2O)_2^+$		$(NH_3)_2^+$	
		D_e	r_e	D_e	r_e	D_e	r_e	D_e	r_e	D_e	r_e	D_e	r_e	D_e	r_e
B3LYP		67.8	1.11	77.6	1.14	59.0	1.81	43.2	2.53	58.1	1.93	52.7	2.10	51.5	2.25
Lh-SVWN	$g_\sigma = 0.48t_\sigma$ ($\sigma = \alpha, \beta$)	65.6	1.09	68.1	1.12	55.4	1.83	41.7	2.51	55.0	1.94	50.2	2.10	49.0	2.25
Lh-SVWN	$g_\alpha = (0.446 + 0.0531\zeta)t_\alpha$ $g_\beta = (0.446 - 0.0531\zeta)t_\beta$	65.6	1.09	68.2	1.12	57.2	1.83	42.7	2.51	56.6	1.93	51.5	2.10	50.1	2.25
Lh-SVWN	$g_\sigma = \mathrm{erf}(0.22s_\sigma)$ ($\sigma = \alpha, \beta$)	66.5	1.11	73.6	1.13	54.8	1.83	41.7	2.50	54.4	1.93	49.6	2.09	48.8	2.24
Lh-SVWN	$g_\alpha = \mathrm{erf}[(0.197 + 0.0423\zeta)s_\alpha]$ $g_\beta = \mathrm{erf}[(0.197 - 0.0423\zeta)s_\beta]$	66.4	1.11	72.9	1.14	57.3	1.83	42.9	2.50	56.5	1.93	51.3	2.09	50.1	2.24
CCSD(T) [b]		64.3	1.06	56.0	1.08	30.8	1.71	29.3[c]	2.42[c]	40.2	1.85	40.8	2.03	36.3	2.17

[a] Results with an uncontracted QZVP basis. Dissociation energies are provided with respect to the correct dissociation limit X + X$^+$. [b] Data from ref 56 (unless noted otherwise). [c] CCSD(T) calculation of the energy at the structure optimized at the MP2 level (ref 55).

TABLE 5: Density-Averaged LMFs, $\Delta\bar{g}$ (eqs 31 and 32), for Open-Shell Atoms and Species from the G2-1 Test Set

atom/radical, multiplicity	*Lh*-SVWN, $g_\sigma =$			
	$0.48t_\sigma$	$(0.446 \pm 0.0531\zeta)t_\sigma$	$\mathrm{erf}(0.22s_\sigma)$	$\mathrm{erf}[(0.197 \pm 0.0423)s_\sigma]$
Li, 2	0.0579	0.0307	0.0235	−0.0046
C, 3	0.0964	0.0665	0.0630	0.0262
N, 4	0.1356	0.0986	0.0885	0.0417
O, 3	0.0929	0.0718	0.0570	0.0295
F, 2	0.0392	0.0303	0.0259	0.0138
Si, 3	0.0138	0.0030	0.0143	−0.0012
P, 4	0.0282	0.0140	0.0254	0.0048
S, 3	0.0274	0.0181	0.0206	0.0072
Cl, 2	0.0141	0.0098	0.0109	0.0045
BeH, 2	0.0405	0.0218	0.0276	0.0070
CH, 2	0.0581	0.0445	0.0312	0.0148
CH_2, 3	0.1126	0.0896	0.0583	0.0304
CH_3, 2	0.0595	0.0488	0.0299	0.0167
ClO, 2	0.0071	0.0044	0.0058	0.0020
CN, 2	0.0103	0.0050	0.0112	0.0033
HCO, 2	0.0103	0.0051	0.0082	0.0013
NH, 3	0.1004	0.0786	0.0576	0.0300
NH_2, 2	0.0470	0.0374	0.0277	0.0152
NO, 2	0.0134	0.0085	0.0098	0.0033
O_2, 3	0.0240	0.0155	0.0197	0.0080
OH, 2	0.0418	0.0327	0.0266	0.0144
PH_2, 2	0.0186	0.0137	0.0119	0.0051
S_2, 3	0.0083	0.0041	0.0084	0.0021
Si_2, 3	0.0157	0.0148	0.0130	0.0062
SiH_2, 3	0.0268	0.0166	0.0177	0.0040
SiH_3, 2	0.0169	0.0115	0.0101	0.0032
SO, 3	0.0121	0.0064	0.0113	0.0031
average	0.0418	0.0297	0.0265	0.0108

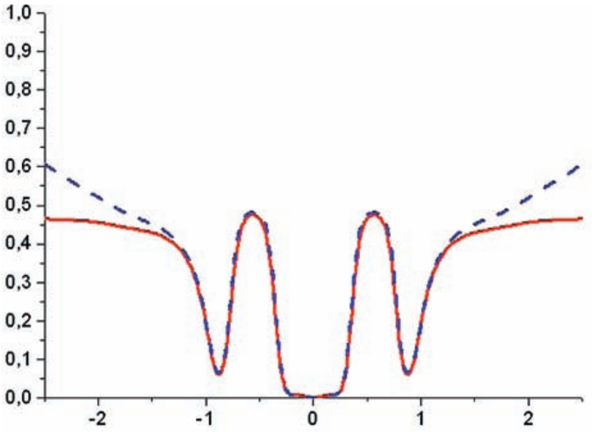

Figure 1. One-dimensional display of local mixing functions for the N_2 molecule (along the internuclear axis, at the equilibrium structure). Solid line: $g = 0.48t$; dashed line: "mixed" LMF $g = 0.48t + 0.52[s/(20 + s)]^2$.

distribution (hopefully without rendering the functional too complicated[26]). As shown here, consideration of explicit real space NDC treatments like the B05 ansatz[32,33] may provide guidelines of how to achieve this goal. Alternatively, a search for computationally more tractable[34] analytical mixing functions for explicit NDC models appears to be a promising avenue.

One point that has so far been viewed as a severe obstacle for the development of accurate local hybrids[29,57] is a mismatch between the gauges of exact and DFT exchange energy densities. The good numerical results of several recent local hybrids may be viewed as an argument against this thesis. Notably, however, almost all successful local hybrids so far used only LSDA and exact exchange,[14,22,23] with no GGA contributions to exchange (but note ref 26). As shown in this work, this may reflect the fact that the LSDA and exact exchange energy densities are already in better matching gauges by definition. The gauge problem is therefore reduced or absent in this case.

Acknowledgment. This work has been funded by Deutsche Forschungsgemeinschaft (Project KA1187/10-1) within Priority Program 1145, "Modern and universal first-principles methods for many-electron systems in chemistry and physics". H.B. thanks the Studienstiftung des deutschen Volkes for a Ph.D. student scholarship. We thank R. Ahlrichs (Karlsruhe) and the Turbomole developer consortium for access to the Turbomole source code. B. Zarzycki is acknowledged for performing some of the calculations.

Appendix

On the Self-Consistent Implementation of Spin-Polarization Dependent Local Hybrids. Occupied-orbital-dependent functionals that explicitly depend on the exact exchange energy density, ε_x^{exact} (eq 8), and/or the local kinetic energy density, τ (eq 12), are implicit rather than explicit functionals of the density. This leads to a well-known problem in their self-consistent implementation as a Kohn-Sham potential cannot be derived directly by taking explicitly the functional derivative with respect to the electron density ($\delta E_{xc}/\delta\rho$). The first step of an implementation will therefore always be the evaluation of functional derivatives with respect to the occupied orbitals (FDOs), $\delta E_{xc}/\delta\varphi_i$. For a functional of the following form (a typical "hyper-GGA" functional without dependence on the density Laplacian[12])

$$E_{xc} = \int \varepsilon_{xc}[\rho_\alpha(\mathbf{r}), \rho_\beta(\mathbf{r}); \nabla\rho_\alpha(\mathbf{r}), \nabla\rho_\beta(\mathbf{r}); \tau_\alpha(\mathbf{r}), \tau_\beta(\mathbf{r}); \varepsilon_{x,\alpha}^{exact}(\mathbf{r}), \varepsilon_{x,\beta}^{exact}(\mathbf{r})]d\mathbf{r} \quad (A1)$$

one can easily show that such FDOs are assembled from partial derivatives $(\partial\varepsilon_{\mathrm{xc}}/\partial\rho_\sigma)$, $(\partial\varepsilon_{\mathrm{xc}}/\partial|\nabla\rho_\sigma|)$, $(\partial\varepsilon_{\mathrm{xc}}/\partial\tau_\sigma)$, and $(\partial\varepsilon_{\mathrm{xc}}/\partial\varepsilon_{\mathrm{x},\sigma}^{\mathrm{exact}})$ $(\sigma = \alpha, \beta)$ as

$$\begin{aligned}\frac{\delta E_{\mathrm{xc}}}{\delta\varphi_{k_\sigma}} = {} & 2\left\{\frac{\partial\varepsilon_{\mathrm{xc}}}{\partial\rho_\sigma} - \frac{\partial\varepsilon_{\mathrm{xc}}}{\partial|\nabla\rho_\sigma|}\left(\frac{\nabla^2\rho_\sigma}{|\nabla\rho_\sigma|} - \frac{\nabla\rho_\sigma\cdot\nabla|\nabla\rho_\sigma|}{|\nabla\rho_\sigma|^2}\right) - \right. \\ & \left. \frac{1}{|\nabla\rho_\sigma|}\left(\nabla\frac{\partial\varepsilon_{\mathrm{xc}}}{\partial|\nabla\rho_\sigma|}\right)\cdot\nabla\rho_\sigma\right\}\varphi_{k_\sigma} \\ & -\left[\left(\nabla\frac{\partial\varepsilon_{\mathrm{xc}}}{\partial\tau_\sigma}\right)\cdot\nabla + \frac{\partial\varepsilon_{\mathrm{xc}}}{\partial\tau_\sigma}\nabla^2\right]\varphi_{k_\sigma} \\ & +\left(\frac{\partial\varepsilon_{\mathrm{xc}}}{\partial\varepsilon_{\mathrm{x},\sigma}^{\mathrm{exact}}}\right)\hat{\mathrm{V}}_{\mathrm{x},\sigma}^{\text{non-loc}}\varphi_{k_\sigma} + \hat{\mathrm{V}}_{\mathrm{x},\sigma}^{\text{non-loc}}\left\{\left(\frac{\partial\varepsilon_{\mathrm{xc}}}{\partial\varepsilon_{\mathrm{x},\sigma}^{\mathrm{exact}}}\right)\varphi_{k_\sigma}\right\}\end{aligned} \tag{A2}$$

where the operator $\hat{\mathrm{V}}_{\mathrm{x},\sigma}^{\text{non-loc}}$ is defined by its action on an arbitrary function ψ as[58]

$$\hat{\mathrm{v}}_{\mathrm{x},\sigma}^{\text{non-loc}}(\mathbf{r})\psi(\mathbf{r}) = -\sum_{j_\sigma}^{\mathrm{occ}}\varphi_{j_\sigma}(\mathbf{r})\int\frac{\varphi_{j_\sigma}^*(\mathbf{r}')\psi(\mathbf{r}')}{|\mathbf{r}-\mathbf{r}'|}\mathrm{d}\mathbf{r}' \tag{A3}$$

It is obvious that in a closed-shell system, for a doubly occupied pair with an identical spatial part (i.e., $\varphi_{i_\alpha} = \varphi_{i_\beta} = \varphi_i$), each of the counterparts φ_{i_α} and φ_{i_β} must enter the expression for E_{xc} equivalently. Otherwise, spurious spin polarization will unavoidably appear during the SCF process. In other words, if $\delta E_{\mathrm{xc}}/\delta\varphi_{i_\alpha}$ is not identical to $\delta E_{\mathrm{xc}}/\delta\varphi_{i_\beta}$, then φ_{i_α} and φ_{i_β} (identical from an initial guess) will necessarily differ already after the first SCF iteration. To ensure that these alpha and beta spin FDOs coincide (cf. eq A2), one has to require that

$$\frac{\partial\varepsilon_{\mathrm{xc}}}{\partial\kappa_\alpha} = \frac{\partial\varepsilon_{\mathrm{xc}}}{\partial\kappa_\beta} \qquad \kappa = \rho, |\nabla\rho|, \tau, \varepsilon_{\mathrm{x}}^{\mathrm{exact}} \tag{A4}$$

On the RHS of eq 19, only the term $E_{\mathrm{NDC}}^{\text{loc-hyb}}$ has to be verified (for the other two terms, eq A4 is satisfied automatically). Let us now substitute LMFs (eq 25) into such a functional (eqs 20)

$$\begin{aligned}E_{\mathrm{NDC}}^{\text{loc-hyb}} = \sum_{\sigma=\alpha,\beta}\int\{1 - F[(b_\sigma + c_\sigma\zeta(\mathbf{r}))\theta_\sigma(\mathbf{r})]\} \times \\ [\varepsilon_{\mathrm{x},\sigma}^{\mathrm{DFT}}(\mathbf{r}) - \varepsilon_{\mathrm{x},\sigma}^{\mathrm{exact}}(\mathbf{r})]\mathrm{d}\mathbf{r} \qquad \theta = t, s\end{aligned} \tag{A5}$$

Then, abbreviating $(\varepsilon_{\mathrm{x},\sigma}^{\mathrm{DFT}} - \varepsilon_{\mathrm{x},\sigma}^{\mathrm{exact}})$ as $\Delta\varepsilon_{\mathrm{x},\sigma}$, we have

$$\begin{aligned}\frac{\partial\varepsilon_{\mathrm{NDC}}^{\text{loc-hyb}}}{\partial\kappa_\sigma} = {} & \{1 - F[(b_\sigma + c_\sigma\zeta)\theta_\sigma]\}\frac{\partial\Delta\varepsilon_{\mathrm{x},\sigma}}{\partial\kappa_\sigma} - \\ & F'[(b_\sigma + c_\sigma\zeta)\theta_\sigma]\left[b_\sigma + c_\sigma\left(\frac{\partial\zeta}{\partial\kappa_\sigma}\theta_\sigma + \zeta\frac{\partial\theta_\sigma}{\partial\kappa_\sigma}\right)\right]\Delta\varepsilon_{\mathrm{x},\sigma} - \\ & F'[(b_{\sigma'} + c_{\sigma'}\zeta)\theta_{\sigma'}]c_{\sigma'}\frac{\partial\zeta}{\partial\kappa_\sigma}\theta_{\sigma'}\Delta\varepsilon_{\mathrm{x},\sigma'} \qquad \sigma' \neq \sigma\end{aligned} \tag{A6}$$

where $F'(z) = (\mathrm{d}F(z)/\mathrm{d}z)$ and $z = (b_\sigma + c_\sigma\zeta)\theta_\sigma$.

The easiest way to justify eq 27a consists of substituting $\kappa = \varepsilon_{\mathrm{x}}^{\mathrm{exact}}$ into eq A6. Indeed, since only $\Delta\varepsilon_{\mathrm{x},\sigma}$ depends (linearly) on $\varepsilon_{\mathrm{x}}^{\mathrm{exact}}$,

$$\frac{\partial\varepsilon_{\mathrm{NDC}}^{\text{loc-hyb}}}{\partial\varepsilon_{\mathrm{x},\sigma}^{\mathrm{exact}}} = -\{1 - F[(b_\sigma + c_\sigma\zeta)\theta_\sigma]\} \tag{A7}$$

Use of $\varphi_{i_\alpha} = \varphi_{i_\beta}$ in the evaluation of ρ_σ, $|\nabla\rho_\sigma|$, and τ_σ, (and $\varepsilon_{\mathrm{x},\sigma}^{\mathrm{exact}}$) obviously leads to $\theta_\beta = \theta_\alpha$ and $\zeta = 0$. Therefore, to satisfy eq A4, one has to put $b_\beta = b_\alpha$. Inspection of eq A6 indicates that the only additional difference upon passing from $\partial\varepsilon_{\mathrm{NDC}}^{\text{loc-hyb}}/\partial\kappa_\alpha$ to $\partial\varepsilon_{\mathrm{NDC}}^{\text{loc-hyb}}/\partial\kappa_\beta$ may arise from $\partial\zeta/\partial\rho_\sigma$ (since ζ depends neither on $|\nabla\rho_\sigma|$ nor on τ_σ). Indeed

$$\frac{\partial\zeta}{\partial\rho_\alpha} = \frac{1-\zeta}{\rho} \quad \text{and} \quad \frac{\partial\zeta}{\partial\rho_\beta} = \frac{-1-\zeta}{\rho} \tag{A8}$$

and, in particular

$$\left.\frac{\partial\zeta}{\partial\rho_\beta}\right|_{\zeta=0} = -\left.\frac{\partial\zeta}{\partial\rho_\alpha}\right|_{\zeta=0} \tag{A9}$$

Therefore, to satisfy eq A4, one has to put $c_\beta = -c_\alpha$ (eq 27b).

References and Notes

(1) Becke, A. D. *J. Chem. Phys.* **1993**, *98*, 5648.

(2) (a) Lee, C.; Yang, W.; Parr, R. G. *Phys. Rev. B* **1988**, *37*, 785. (b) Miehlich, B.; Savin, A.; Stoll, H.; Preuss, H. *Chem. Phys. Lett.* **1989**, *157*, 200.

(3) Stephens, P. J.; Devlin, F. J.; Chabalowski, C. F.; Frisch, M. J. *J. Phys. Chem.* **1994**, *98*, 11623.

(4) (a) Dirac, P. A. M. *Proc. Cambridge Philos. Soc.* **1930**, *26*, 376. (b) Slater, J. C. *Phys. Rev.* **1951**, *81*, 385.

(5) Von Barth, U.; Hedin, L. *J. Phys. C* **1972**, *5*, 1629.

(6) Vosko, S. J.; Wilk, L.; Nusair, M. *Can. J. Phys.* **1980**, *58*, 1200.

(7) Perdew, J. P. *Phys. Rev. Lett.* **1985**, *55*, 1665.

(8) Perdew, J. P.; Yue, W. *Phys. Rev. B* **1986**, *33*, 8800.

(9) Perdew, J. P. *Phys. Rev. B* **1986**, *33*, 8822.

(10) Becke, A. D. *Phys. Rev. A* **1988**, *38*, 3098.

(11) Becke, A. D. *J. Chem. Phys.* **1996**, *104*, 1040.

(12) Perdew, J. P.; Schmidt K. *Density Functional Theory and its Application to Materials*, AIP Conference Proceedings, Vol. 577; van Doren, V., van Alsenoy, C., Geerlings, P., Eds.; AIP: Melville, NY, 2001; pp 1−20.

(13) Jaramillo, J.; Scuseria, G. E.; Ernzerhof, M. *J. Chem. Phys.* **2003**, *118*, 1068.

(14) Kaupp, M.; Bahmann, H.; Arbuznikov, A. V. *J. Chem. Phys.* **2007**, *127*, 194102.

(15) Gritsenko, O. V.; Schipper, P. R. T.; Baerends, E. J. *J. Chem. Phys.* **1997**, *107*, 5007.

(16) We do not consider here other parameters, hidden sometimes inside of $\tilde{E}_{\mathrm{xc}}^{\mathrm{DFT}}$; they may lack physical justification but can provide some extra flexibility of the functionals.

(17) Perdew, J. P.; Ernzerhof, M.; Burke, K. *J. Chem. Phys.* **1996**, *105*, 9982.

(18) (a) Durant, J. L. *Chem. Phys. Lett.* **1996**, *256*, 595. (b) Chermette, H.; Razafinjanahary, H.; Carrion, L. *J. Chem. Phys.* **1997**, *107*, 10643.

(19) (a) Munzarová, M.; Kaupp, M. *J. Phys. Chem. A* **1999**, *103*, 9966. (b) Wilson, P. J.; Amos, R. D.; Handy, N. C. *Chem. Phys. Lett.* **1999**, *312*, 475. (c) Bühl, M.; Kaupp, M.; Malkin, V. G.; Malkina, O. L. *J. Comput. Chem.* **1999**, *20*, 91. (d) Wilson, P. J.; Tozer, D. J. *J. Chem. Phys.* **2002**, *116*, 10139. (e) Kaupp, M.; Reviakine, R.; Malkina, O. L.; Arbuznikov, A. V.; Schimmelpfennig, B.; Malkin, V. G. *J. Comput. Chem.* **2002**, *23*, 794. (f) Arbuznikov, A. V.; Kaupp, M. *Chem. Phys. Lett.* **2004**, *386*, 8. (g) Arbuznikov, A. V.; Kaupp, M. *Chem. Phys. Lett.* **2004**, *391*, 16. (h) Champagne, B.; Botek, E.; Nakano, M.; Nitta, T.; Yamaguchi, K. *J. Chem. Phys.* **2005**, *122*, 114315. (i) Miura, M.; Aoki, Y.; Champagne, B. *J. Chem. Phys.* **2007**, *127*, 084103.

(20) (a) Leininger, T.; Stoll, H.; Werner, H.-J.; Savin, A. *Chem. Phys. Lett.* **1997**, *275*, 151. (b) Iikura, H.; Tsuneda, T.; Yanai, T.; Hirao, K. *J. Chem. Phys.* **2001**, *115*, 3540. (c) Yanai, T.; Tew, D. P.; Handy, N. C. *Chem. Phys. Lett.* **2004**, *393*, 51. (d) Gerber, I. C.; Angyan, J. G. *Chem. Phys. Lett.* **2005**, *415*, 100. (e) Baer, R.; Neuhauser, D. *Phys. Rev. Lett.* **2005**, *94*, 043002. (f) Vydrov, O. A.; Heyd, J.; Krukau, A. V.; Scuseria, G. E. *J. Chem. Phys.* **2006**, *125*, 074106.

(21) Cruz, F. G.; Lam, K.-C.; Burke, K. *J. Phys. Chem. A* **1998**, *102*, 4911.

(22) Bahmann, H.; Rodenberg, A.; Arbuznikov, A. V.; Kaupp, M. *J. Chem. Phys.* **2007**, *126*, 011103.

(23) Arbuznikov, A. V.; Kaupp, M. *Chem. Phys. Lett.* **2007**, *440*, 160.

(24) Janesko, B. G.; Scuseria, G. E. *J. Chem. Phys.* **2007**, *127*, 164117.

(25) Arbuznikov, A. V.; Kaupp, M. *J. Chem. Phys.* **2008**, *128*, 214107.

(26) Perdew, J. P.; Staroverov, V. N.; Tao, J.; Scuseria, G. E. *Phys. Rev. A* **2008**, *78*, 052513.

(27) Burke, K.; Cruz, F. G.; Lam, K.-C. *J. Chem. Phys.* **1998**, *109*, 8161.

(28) Burke, K.; Cruz, F. G.; Lam, K.-C. *Int. J. Quantum Chem.* **1998**, *70*, 583.

(29) Tao, J.; Staroverov, V. N.; Scuseria, G. E.; Perdew, J. P. *Phys. Rev. A* **2008**, *77*, 012509.

(30) The effect of such a calibration on other properties (not related to the total energy) has not yet been investigated.

(31) Arbuznikov, A. V.; Kaupp, M. *Chem. Phys. Lett.* **2007**, *442*, 496.

(32) Becke, A. D. *J. Chem. Phys.* **2003**, *119*, 2972.

(33) Becke, A. D. *J. Chem. Phys.* **2005**, *122*, 064101.

(34) Arbuznikov, A. V.; Kaupp, M. Submitted.

(35) See eqs 20−26 and the Appendix of ref 32.

(36) See eqs 19−23 and the Appendix of ref 33. In our notation, $B_\sigma = -A_{\sigma\sigma} M_\sigma^{(1)}/2$.

(37) Parr, R. G.; Yang, W. *Density-Functional Theory of Atoms and Molecules*; Oxford University Press: New York, 1989.

(38) Malkin, V. G.; Malkina, O. L.; Reviakine, R.; Arbuznikov, A. V.; Kaupp, M.; Schimmelpfennig, B.; Malkin, I.; Repiský, M.; Komorovský, S.; Hrobarik, P.; Malkin, E.; Helgaker, T.; Ruud, K. *ReSpect program*, version 2.1; 2008.

(39) Turbomole 5.10; See, for example: (a) Ahlrichs, R.; Baer, M.; Haeser, M.; Horn, H.; Koelmel, C. *Chem. Phys. Lett.* **1989**, *162*, 165. (b) Treutler, O.; Ahlrichs, R. *J. Chem. Phys.* **1995**, *102*, 346.

(40) (a) Dunning, T. H., Jr. *J. Chem. Phys.* **1989**, *90*, 1007. (b) Woon, D. E.; Dunning, T. H., Jr. *J. Chem. Phys.* **1993**, *98*, 1358.

(41) Weigend, F.; Ahlrichs, R. *Phys. Chem. Chem. Phys.* **2005**, *7*, 3297.

(42) In the ReSpect implementation, a separate uncontraction step for the orbital basis had been inserted to minimize errors arising from the resolution of the identity in the calculation of the exact exchange energy density; see: Arbuznikov, A. V.; Kaupp, M.; Bahmann, H. *J. Chem. Phys.* **2006**, *124*, 204102. In the new Turbomole-based implementation, this has so far not been done as it is planned to exploit other means to improve efficiency.

(43) Overall, the results presented here are quite insensitive to the choice of orbitals.

(44) Lynch, B. J.; Truhlar, D. G. *J. Phys. Chem. A* **2003**, *107*, 8996.

(45) Mean absolute errors for AEs and BHs are minimized simultaneously, on equal footing.

(46) (a) Pople, J. A.; Head-Gordon, M.; Fox, D. J.; Raghavachari, K.; Curtiss, L. A. *J. Chem. Phys.* **1989**, *90*, 5622. (b) Curtiss, L. A.; Jones, C.; Trucks, G. W.; Raghavachari, K.; Pople, J. A. *J. Chem. Phys.* **1990**, *93*, 2537.

(47) Della Sala, F.; Görling, A. *J. Chem. Phys.* **2001**, *115*, 5718.

(48) Curtiss, L. A.; Raghavachari, K.; Redfern, P. C.; Pople, J. A. *J. Chem. Phys.* **1997**, *106*, 1063.

(49) Curtiss, L. A.; Raghavachari, K.; Redfern, P. C.; Rassolov, V.; Pople, J. A. *J. Chem. Phys.* **1998**, *109*, 7764.

(50) Curtiss, L. A.; Raghavachari, K.; Redfern, P. C.; Pople, J. A. *J. Chem. Phys.* **2000**, *112*, 7374.

(51) Zhao, Y.; Lynch, B. J.; Truhlar, D. G. *Phys. Chem. Chem. Phys.* **2005**, *7*, 43.

(52) Zhao, Y.; González-García, N.; Truhlar, D. G. *J. Phys. Chem. A* **2005**, *109*, 2012.

(53) (a) Grimme, S. *J. Chem. Phys.* **2006**, *124*, 034108. (b) Schwabe, T.; Grimme, S. *Phys. Chem. Chem. Phys.* **2007**, *9*, 3397.

(54) Grüning, M.; Gritsenko, O. V.; van Gisbergen, S. J. A.; Baerends, E. J. *J. Phys. Chem. A* **2001**, *105*, 9211.

(55) Braïda, B.; Hilberty, P. C.; Savin, A. *J. Phys. Chem. A* **1998**, *102*, 7872.

(56) Gräfenstein, J.; Kraka, E.; Cremer, D. *Phys. Chem. Chem. Phys.* **2004**, *6*, 1096.

(57) Furche, F.; Rappoport, D. *Nachr. Chem.* **2009**, *57*, 305.

(58) The first and second (combined), third, and fourth lines of the RHS of eq A2 represent local and multiplicative, local but nonmultiplicative, and, finally, nonlocal and nonmultiplicative contributions to the FDO, respectively.

JP903233Q